

Morphotropic phase boundary and electric properties in $(1-x)\text{Bi}_0.5\text{Na}_0.5\text{TiO}_3-x\text{BiCoO}_3$ lead-free piezoelectric ceramics

Fei-Fei Guo, Bin Yang, Shan-Tao Zhang, Xiao Liu, Li-Mei Zheng et al.

Citation: *J. Appl. Phys.* **111**, 124113 (2012); doi: 10.1063/1.4730770

View online: <http://dx.doi.org/10.1063/1.4730770>

View Table of Contents: <http://jap.aip.org/resource/1/JAPIAU/v111/i12>

Published by the [American Institute of Physics](#).

Related Articles

Structural diversity of the $(\text{Na}_{1-x}\text{K}_x)_0.5\text{Bi}_0.5\text{TiO}_3$ perovskite at the morphotropic phase boundary
J. Appl. Phys. **113**, 024106 (2013)

First-principles based multiscale model of piezoelectric nanowires with surface effects
J. Appl. Phys. **113**, 014309 (2013)

Large decrease of characteristic frequency of dielectric relaxation associated with domain-wall motion in Sb^{5+} -modified $(\text{K},\text{Na})\text{NbO}_3$ -based ceramics
Appl. Phys. Lett. **101**, 252905 (2012)

Enhanced piezoelectric performance from carbon fluoropolymer nanocomposites
J. Appl. Phys. **112**, 124104 (2012)

Reduction of the piezoelectric performance in lead-free $(1-x)\text{Ba}(\text{Zr}_{0.2}\text{Ti}_{0.8})\text{O}_3-x(\text{Ba}_{0.7}\text{Ca}_{0.3})\text{TiO}_3$ piezoceramics under uniaxial compressive stress
J. Appl. Phys. **112**, 114108 (2012)

Additional information on *J. Appl. Phys.*

Journal Homepage: <http://jap.aip.org/>

Journal Information: http://jap.aip.org/about/about_the_journal

Top downloads: http://jap.aip.org/features/most_downloaded

Information for Authors: <http://jap.aip.org/authors>

ADVERTISEMENT



AIP Advances

Now Indexed in Thomson Reuters Databases

Explore AIP's open access journal:

- Rapid publication
- Article-level metrics
- Post-publication rating and commenting

Morphotropic phase boundary and electric properties in $(1-x)\text{Bi}_{0.5}\text{Na}_{0.5}\text{TiO}_3-x\text{BiCoO}_3$ lead-free piezoelectric ceramics

Fei-Fei Guo,¹ Bin Yang,^{1,a)} Shan-Tao Zhang,^{2,b)} Xiao Liu,¹ Li-Mei Zheng,¹ Zhu Wang,¹ Feng-Min Wu,¹ Da-Li Wang,³ and Wen-Wu Cao^{1,4}

¹Department of Physics, Center for Condensed Matter Science and Technology, Harbin Institute of Technology, Harbin 150001, China

²Department of Materials Science and Engineering & National Laboratory of Solid State Microstructures, Nanjing University, Nanjing 210093, China

³School of Chemical Engineering and Technology, Harbin Institute of Technology, Harbin 150001, China

⁴Materials Research Institute, The Pennsylvania State University, University Park, Pennsylvania 16802, USA

(Received 11 September 2011; accepted 26 May 2012; published online 26 June 2012)

Lead-free $(1-x)\text{Bi}_{0.5}\text{Na}_{0.5}\text{TiO}_3-x\text{BiCoO}_3$ ($x = 0, 0.015, 0.025, 0.03, 0.035, 0.04, \text{ and } 0.06$) piezoelectric ceramics have been synthesized and their structure and electric properties have been investigated systemically. The rhombohedral-tetragonal morphotropic phase boundary (MPB) locates near $x = 0.025\text{--}0.035$. For the ceramics with $x = 0.025$, the saturated polarization (P_s), remnant polarization (P_r), coercive field (E_c), strain (S), piezoelectric constant (d_{33}), and thickness electromechanical coupling factor (k_t) are $40.6 \mu\text{C}/\text{cm}^2$, $35.4 \mu\text{C}/\text{cm}^2$, $5.25 \text{ kV}/\text{mm}$, 0.11% , $107 \text{ pC}/\text{N}$, and 0.45 , respectively. The low temperature humps of relative dielectric constant, which is indicative of T_{R-T} , are becoming inconspicuous gradually with the increasing x and almost disappear at $x = 0.04$. The depolarization temperature T_d decreases first and then increases with the increasing x . Our results may be helpful for further work on $\text{Bi}_{0.5}\text{Na}_{0.5}\text{TiO}_3$ -based lead-free piezoelectric ceramics. © 2012 American Institute of Physics. [<http://dx.doi.org/10.1063/1.4730770>]

I. INTRODUCTION

Lead-based piezoelectric ceramics exemplified by $\text{Pb}(\text{Zr,Ti})\text{O}_3$ (PZT) are widely used for sensors, actuators, and ultrasonic motors in virtue of their excellent piezoelectric properties.^{1,2} However, in recent years, lead-pollution and environmental problems caused by the use of lead-containing piezoelectric materials have become increasingly serious because of the toxicity of lead oxides. From the perspective of environmental protection, it is necessary to develop high performance lead-free piezoelectric materials to replace the lead-based counterparts.

$\text{Bi}_{0.5}\text{Na}_{0.5}\text{TiO}_3$ (BNT) and its solid solutions with other perovskites can have good piezoelectric properties and thus BNT-based materials are considered to be the potential candidates for replacing PZT. Pure BNT is an A-site complex perovskite-structured ferroelectrics with a relative high Curie temperature ($T_c = 320^\circ\text{C}$).³ At room temperature, BNT has a rhombohedral symmetry with strong ferroelectricity ($P_r = 38 \mu\text{C}/\text{cm}^2$).^{4,5} However, the poling treatment of pure BNT ceramic is very difficult because of its high coercive field ($E_c = 7.3 \text{ kV}/\text{mm}$), resulting in relatively weak piezoelectric properties ($d_{33} \sim 73\text{--}80 \text{ pC}/\text{N}$). In order to decrease coercive field and improve the poling process, forming BNT-based solid solution with a morphotropic phase boundary (MPB) as an effective way has been proposed and studied. Similar to PZT, piezoelectric properties of BNT-based solid solution also show maximum

values near the MPBs. The anomalously high piezoelectric performance based on the fact that, the composition-induced ferro-ferro transition at MPB causes the instability of the polarization state so that the polarization direction can be easily rotated by external stress or electric field.^{6,7} Up to now, many binary or ternary BNT-based MPBs have been reported.^{5,8–15} The reported BNT-based MPBs are generally formed by rhombohedral BNT and cubic/tetragonal ferroelectrics, and the effect of c/a ratio of the tetragonal end members has not been clearly considered. Actually, for tetragonal ferroelectrics, the c/a ratio plays an important role in determining ferroelectric polarization. Therefore, it may be interesting to investigate BNT-based MPBs formed by BNT and tetragonal ferroelectrics with high c/a ratio.

It is noticed that BiCoO_3 (BC) has a tetragonal symmetry and a large lattice c/a ratio of 1.27 ,¹⁶ which indicating a high ferroelectric polarization. In addition, BC have large polarization $179 \mu\text{C}/\text{cm}^2$ and very high Curie temperature $800\text{--}900 \text{ K}$.^{16,17} Following the above statement, new solid solutions of rhombohedral BNT and tetragonal BC have been supposed. It is anticipated that solid solutions of BNT and BC have a rhombohedral-tetragonal MPB which may improve the piezoelectric properties. In addition, BC are multiferroics with both ferroelectric and antiferromagnetic orders simultaneously,¹⁷ which means introducing BC into BNT may be a positive way to develop multiferroic materials, at least be helpful for further work on BC-based multiferroics. In this study, $(1-x)\text{BNT}-x\text{BC}$ ceramics have been synthesized and their structure and electric properties have been studied.

^{a)}Electronic mail: binyang@hit.edu.cn.

^{b)}Electronic mail: stzhang@mail.nju.edu.cn.

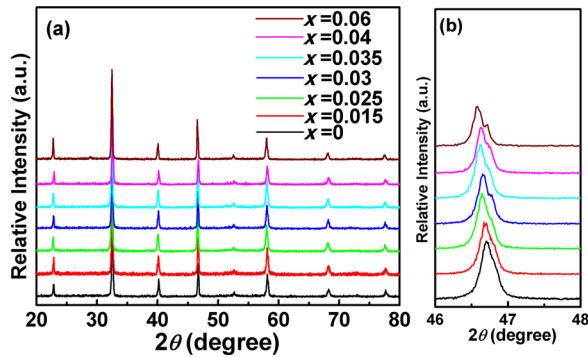


FIG. 1. (a) XRD patterns of $(1-x)\text{BNT}-x\text{BC}$ ceramics, (b) the detailed XRD patterns show the composition induced phase transition, the rhombohedral-tetragonal MPB can be determined to locate near $x = 0.025\text{--}0.035$.

II. EXPERIMENTAL PROCEDURE

Ceramic specimens of $(1-x)\text{BNT}-x\text{BC}$ ($x = 0, 0.015, 0.025, 0.03, 0.035, 0.04, \text{ and } 0.06$) were prepared by conventional solid state reaction method. Reagent grade oxide or carbonate powders of Bi_2O_3 ($\geq 99.0\%$), Na_2CO_3 ($\geq 99.8\%$), TiO_2 ($\geq 99.0\%$), and Co_2O_3 ($\geq 99.0\%$) were used as the starting raw materials. Stoichiometric amounts of the starting reagents were ball-milled for 12 h in ethanol and dried at 100°C . Then the dried well-ground stoichiometric mixtures of the starting reagents were calcined at 820°C for 3 h in open crucibles, and again ball-milled for 24 h. The resulting mixtures were mixed with polyvinyl alcohol as a binder and then pressed into disks of 13 mm in diameter and 1.2 mm in thickness under pressure of 250 MPa. Following binder burn-out at 550°C , the pellets were sintered at 1100°C for 3 h in covered alumina crucibles. In order to reduce the volatility of Bi and Na, the disks were embedded in the same compositional powder during sintering. Prior to the electrical measurements, the pellets were polished to smooth and parallel surfaces. After polishing, the circular surfaces of the disks were covered with a thin layer of silver paste and fired at 550°C for 30 min. The specimens for measurement of piezoelectric properties were poled in silicon oil at room temperature under $7\text{--}8\text{ kV/mm}$ for 15 min.

The crystal structure of the sintered ceramics was determined by x-ray diffraction (XRD) with a Cu $K\alpha$ radiation.

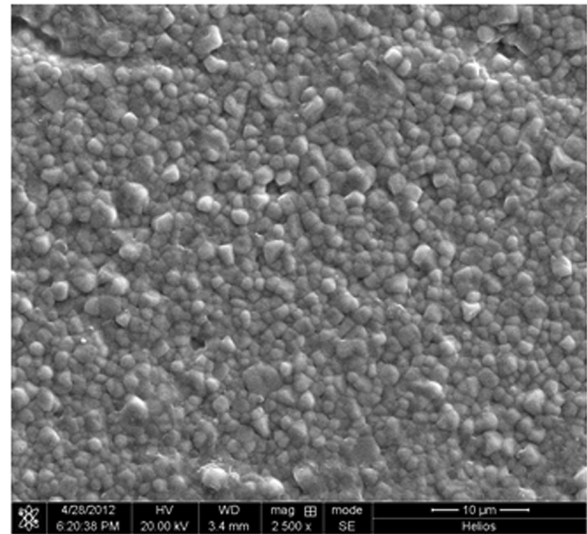


FIG. 2. Typical SEM images of the composition with $x = 0.025$.

The microstructure was examined by a scanning electron microscope (SEM). Temperature dependence of dielectric properties were measured on poled ceramics with a LCR meter (Agilent, E4980A) from room temperature to 450°C with varying frequencies from 1 kHz to 100 kHz. The polarization and strain versus electric field loops of the ceramics were measured at 1 Hz by precision premier II (Radiant Tech. USA) at room temperature in silicone oil. Piezoelectric constant d_{33} of the ceramics was measured by a quasistatic d_{33} meter (Institute of Acoustics, Chinese Academy of Sciences, ZJ-4 A, China). The electromechanical coupling factors k_p and k_t were determined by a resonance-antiresonance method using an impedance analyzer (Agilent 4294 A).

III. RESULTS AND DISCUSSION

The XRD patterns of the $(1-x)\text{BNT}-x\text{BC}$ ceramics are shown in Fig. 1(a). Since no second phase is observed in Fig. 1(a), we conclude that all the samples have the pure perovskite structure. Fig. 1(b) plots the detailed XRD patterns in the 2θ range of $45.5^\circ\text{--}48.0^\circ$. As x increases from 0 to 0.06, the samples with composition $x = 0$ and $x = 0.015$, there are no observable peak splitting, indicating that these two

TABLE I. Lattice parameters of the $(1-x)\text{BNT}-x\text{BC}$ system.

Specimen	Symmetry	Lattice parameter volumes			Unit cell Vol (nm^3)
		a (nm)	c (nm)	α ($^\circ$)	
BNT	R	0.38687	...	89.4(1)	0.05789
0.985BNT-0.015BC	R	0.38903	...	89.8(5)	0.05888
0.975BNT-0.025BC	R	0.38929	...	89.8(7)	0.05900
	T	0.38912	0.38973	...	0.05901
0.97BNT-0.03BC	R	0.38953	...	89.8(7)	0.05911
	T	0.38934	0.38996	...	0.05911
0.965BNT-0.035BC	R	0.38963	...	89.8(7)	0.05915
	T	0.38938	0.39014	...	0.05915
0.96BNT-0.04BC	T	0.38941	0.39037	...	0.05920
0.94BNT-0.06BC	T	0.38946	0.39064	...	0.05925

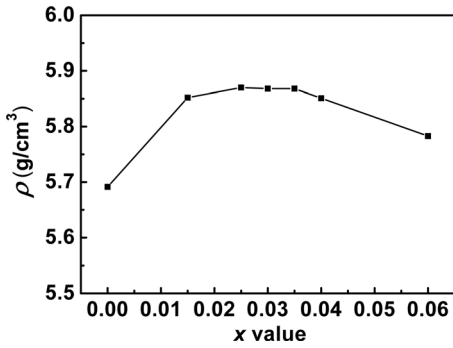


FIG. 3. Density of ceramics as function of BC concentration.

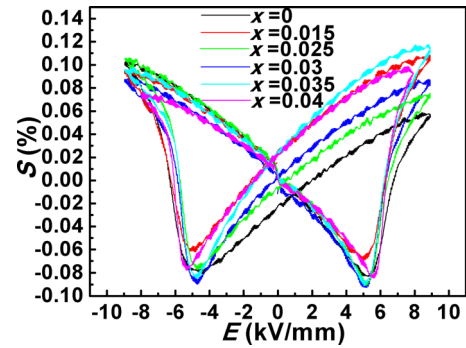


FIG. 5. Bipolar *S-E* curves of the poled ceramics.

compositions have a pure rhombohedral symmetry. With further increasing *x*, the (202) peak tends to split and the splitting becomes more and more obvious, suggesting that a new tetragonal phase appears. When *x* = 0.06, only (002) and (200) peaks are present in the Fig. 1(b), demonstrating the sample with this composition possesses the pure tetragonal phase. In view of above results and following electrical properties, the rhombohedral-tetragonal MPB may be formed near 0.025 ≤ *x* ≤ 0.035 in (1-*x*)BNT-*x*BC system.

The evolution of lattice parameters of (1-*x*)BNT-*x*BC system calculated by the XRD patterns is shown in Table I. It is observed that the lattice parameters increase with increasing the amount of BC in the compositions. This implies that the Co³⁺ ion (*R*_{Co³⁺} = 0.65 Å) with larger ionic radii has diffused into the BNT lattice (*R*_{Ti⁴⁺} = 0.61 Å) and results in the enlargement of lattice. On the other hand, the refinement of the rhombohedral and tetragonal structures for the MPB compositions gave similar unit cell volumes, demonstrating that the coexistence of both phases is plausible for *x* = 0.025, *x* = 0.03, and *x* = 0.035.¹⁸

Fig. 2 shows the SEM micrographs of the composition with *x* = 0.025, which is typical for all compositions. The

dense and homogeneous microstructures are observed, and the average grain size is about 1 μm. No significant composition dependence of grain size can be observed. Fig. 3 shows the density variation as a function of the BC concentration. With the increasing *x* from 0 to 0.06, the density increases and reaches maximum value at *x* = 0.025, then decreases with further addition. The relative densities of all the compositions are between 95.3% and 98.3% compared with theoretical density 5.970 g/cm³.¹⁹

Fig. 4(a) presents the room temperature polarization-electric field (*P-E*) hysteresis loops of all the (1-*x*)BNT-*x*BC ceramics. As can be seen, all ceramics have well-saturated *P-E* hysteresis loops. To further analyse the loops, the detailed composition dependence of saturated polarization (*P*_{*s*}), remnant polarization (*P*_{*r*}), and coercive field (*E*_{*c*}) are plotted in Fig. 4(b). Clearly, the change of the *P*_{*s*} and *P*_{*r*} as functions of *x* value remains entirely consistent. For *x* ≤ 0.025, the *P*_{*s*} and *P*_{*r*} show a tendency to increase slightly with increasing *x*, reaching the maximum values of *P*_{*s*} = 40.6 μC/cm² and *P*_{*r*} = 35.4 μC/cm², and then with the further increasing *x*, both decrease monotonously, with a sharp decrease appears as *x* = 0.04. On the other hand, *E*_{*c*} decreases monotonously with *x* increasing from 0 to 0.06, except for abnormal increase near *x* = 0.04. The ceramics with composition *x* = 0.04 possesses a relatively high *E*_{*c*} and small *P*_{*r*}, indicating that the composition with *x* = 0.04 is out of the MPB region.

Bipolar strain-electric field curves of poled (1-*x*)BNT-*x*BC ceramics are shown in Fig. 5. The typical butterfly shapes are observed for all the samples, indicating the

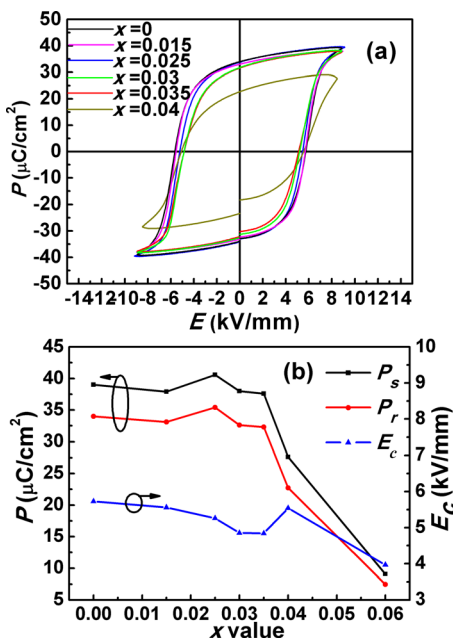


FIG. 4. (a) *P-E* hysteresis loops of (1-*x*)BNT-*x*BC ceramics at room temperature and (b) *P*_{*s*}, *P*_{*r*}, and *E*_{*c*} as functions of *x*.

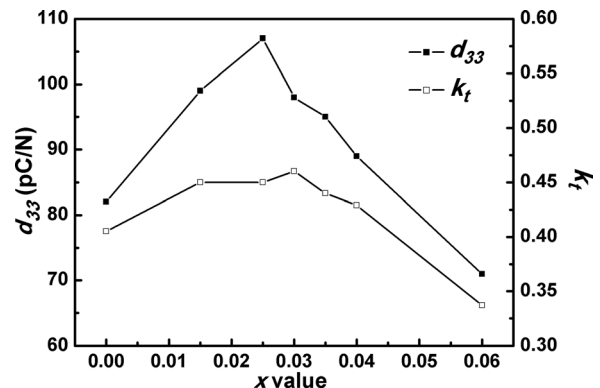


FIG. 6. Composition-dependent *d*₃₃ and *k*_{*t*} for the (1-*x*)BNT-*x*BC ceramics.

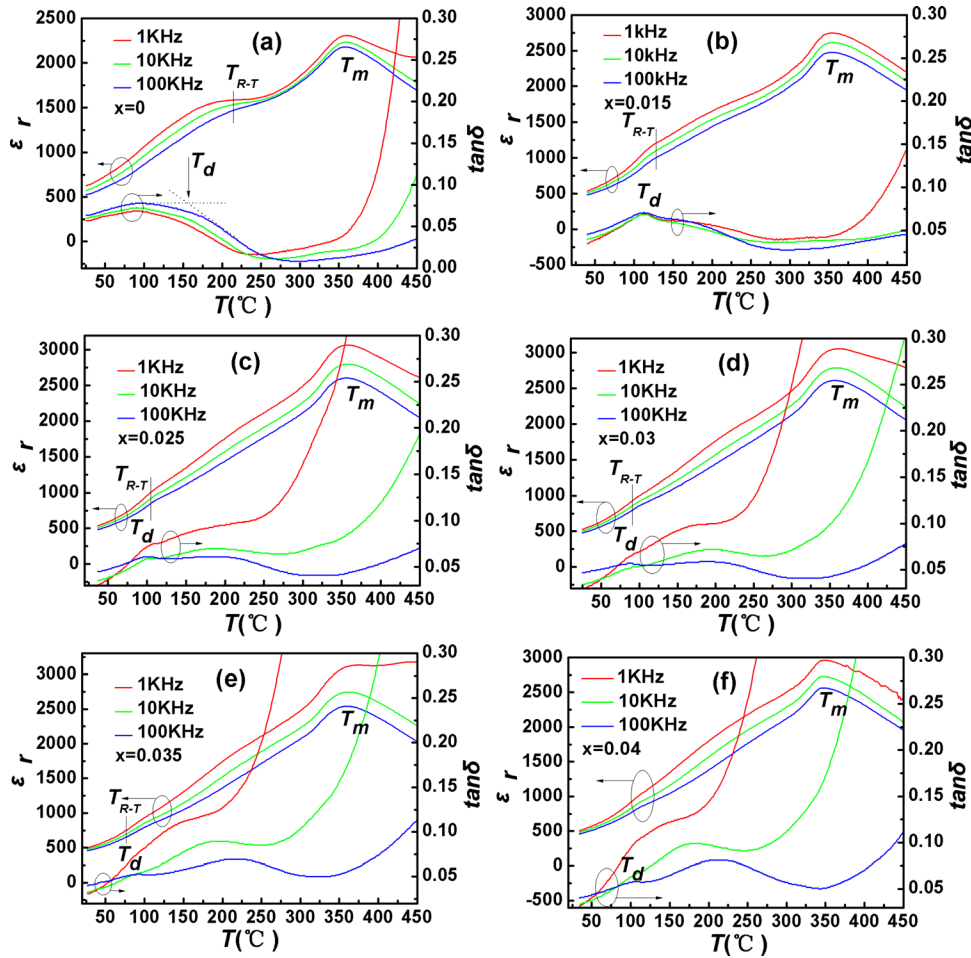


FIG. 7. Temperature dependences of poled relative dielectric constant and loss tangent for $(1-x)\text{BNT}-x\text{BC}$ ceramics.

ferroelectric nature. The maximum positive strain can reach 0.12% for the composition with $x = 0.035$.

Fig. 6 shows the variations of the piezoelectric constant d_{33} and the thickness electromechanical coupling factor k_t with x for $(1-x)\text{BNT}-x\text{BC}$ ceramics. It is found that d_{33} and k_t have a similar variation increasing first and then decreasing with the increasing x . The maximum d_{33} and k_t are 107 pC/N and 0.46, respectively. These results are comparable with other BNT-based solid solution systems. It is noted that the planar electromechanical coupling factor k_p of the ceramics is approximately 0.13–0.145, except for the sample with $x = 0.06$ has a lower k_p value of 0.09, the lower k_p might be related to the poling treatments.

The relative dielectric constant (ϵ_r) and loss tangent ($\tan\delta$) of poled $(1-x)\text{BNT}-x\text{BC}$ ceramics as the functions of temperature are shown in Fig. 7. The depolarization temperature T_d , rhombohedral-tetragonal phase transition temperature T_{R-T} , and the temperature T_m of the maximum dielectric constant were observed. All samples exhibit broad and frequency dependent dielectric peaks, indicating that the ceramics are relaxor ferroelectrics.

According to the report of Hiruma *et al.*,³ the T_d , T_{R-T} , and T_m could be determined from the peak of loss tangent, the low and high temperature hump of relative dielectric constant of the poled samples, respectively. The following should be addressed for Fig. 7: First, the T_d decreases from 157 °C for the composition with $x = 0$ to 87 °C for that with $x = 0.035$, and then tends to increase with further increasing

x . Second, the low temperature humps of relative dielectric constant, which is indicative of the T_{R-T} , are becoming inconspicuous gradually with the increasing x and almost disappear at $x = 0.04$. This observation is consistent with other reports that the B-site substituting of Co^{3+} in BNT system can lead to the low temperature humps of ϵ_r disappear.^{20,21} In other word, the introduction of BC leads to lower T_{R-T} . Third, the T_m values are almost x -independent with the constant values of about 357 °C. It can also be seen that the values of ϵ_r at T_m for BNT-BC solid solutions are higher than those of pure BNT ceramics. And finally, a broaden hump of loss tangent and relative dielectric constant around 200 °C can be seen for all BNT-BC solid solutions whereas it is absent in pure BNT ceramics, which can be attributed to that of the antiferromagnetic-paramagnetic transition of BC.^{16,17} Further works on the magnetic property of this system are underway.

IV. CONCLUSION

In summary, BNT-based solid solution BNT-BC lead-free piezoelectric ceramics were prepared and their structure and electric properties were studied. The MPB of rhombohedral and tetragonal phases was detected in the range of $x = 0.025$ –0.035 by XRD. The electric properties of ceramics with MPB compositions have been improved and the optimum value of d_{33} , k_t , P_s , P_r , E_c , and S for the ceramics with $x = 0.025$ are 107 pC/N, 0.45, 40.6 $\mu\text{C}/\text{cm}^2$, 35.4 $\mu\text{C}/\text{cm}^2$,

5.25 kV/mm, and 0.11%, respectively. The low temperature humps of relative dielectric constant, which is indicative of T_{R-T} , are becoming inconspicuous gradually with the increasing x and almost disappear at $x=0.04$. The depolarization temperature T_d decreases first and then increases with the increasing x . The results may be helpful for further work on BNT-based lead-free piezoelectric ceramics and even for multiferroic materials.

ACKNOWLEDGMENTS

This work was supported by the National Nature Science Foundation of China (10704021, 51102062, and 11174127), the Key Scientific and Technological Project of Harbin (Grant No. 2009AA3BS131), the Postdoctoral Foundation of Heilongjiang Province (Grant No. LBH-Z10147), and the Fundamental Research Funds for the Central Universities (Grant No. HIT. NSRIF. 2011011).

¹G. H. Haertling, *J. Am. Ceram. Soc.* **82**, 797 (1999).

²J. Rödel, W. Jo, K. T. P. Seifert, E.-M. Anton, and T. Granzow, *J. Am. Ceram. Soc.* **92**, 1153 (2009).

³Y. Hiruma, H. Nagata, and T. Takenaka, *J. Appl. Phys.* **104**, 124106 (2008).

⁴G. A. Smolenskii, V. A. Isupov, A. I. Agranovskaya, and N. N. Krainik, *Sov. Phys. Solid State* **2**, 2651 (1961).

⁵T. Takenak, K. Maruyama, and K. Sakata, *Jpn. J. Appl. Phys. Part 1* **30**, 2236 (1991).

⁶H. X. Fu and R. E. Cohen, *Nature (London)* **403**, 281 (2000).

⁷M. Ahart, M. Somayazulu, R. E. Cohen, P. Ganesh, P. Dera, H. K. Mao, R. J. Hemley, Y. Ren, P. Liermann, and Z. G. Wu, *Nature (London)* **451**, 7178, (2008).

⁸K. Sakata, T. Takenaka, and Y. Naitou, *Ferroelectrics* **131**, 219 (1992).

⁹A. B. Kounga, S. T. Zhang, W. Jo, T. Granzow, and J. Rödel, *Appl. Phys. Lett.* **92**, 222902 (2008).

¹⁰A. Sasaki, T. Chiba, Y. Mamiya, and E. Otsuki, *Jpn. J. Appl. Phys. Part 1* **38**, 5564 (1999).

¹¹S. T. Zhang, F. Yan, and B. Yang, *J. Appl. Phys.* **107**, 114110 (2010).

¹²H. Nagata, M. Yoshida, Y. Makiuchi, and T. Takenaka, *Jpn. J. Appl. Phys. Part 1* **42**, 7401 (2003).

¹³X. X. Wang, X. G. Tang, and H. L. W. Chan, *Appl. Phys. Lett.* **85**, 91 (2004).

¹⁴G. F. Fan, W. Z. Lu, X. H. Wang, and F. Liang, *Appl. Phys. Lett.* **91**, 202908 (2007).

¹⁵S. T. Zhang, F. Yan, B. Yang, and W. W. Cao, *Appl. Phys. Lett.* **97**, 122901 (2010).

¹⁶A. A. Belik, S. Iikubo, K. Kodama, N. Igawa, S. Shamoto, S. Niitaka, M. Azuma, Y. Shimakawa, M. Takano, F. Izumi, and E. Takayama-Muromachi, *Chem. Mater.* **18**, 798 (2006).

¹⁷K. Oka, M. Azuma, W. T. Chen, H. Yusa, A. A. Belik, E. Takayama-Muromachi, M. Mizumaki, N. Ishimatsu, N. Hiraoka, M. Tsujimoto, M. G. Tucker, J. P. Attfield, and Y. Shimakawa, *J. Am. Chem. Soc.* **132**, 9438 (2010).

¹⁸S. Zhang, R. Xia, H. Hao, H. Liu, and T. R. Shrout, *Appl. Phys. Lett.* **92**, 152904 (2008).

¹⁹Y. Hiruma, H. Nagata, and T. Takenaka, *J. Appl. Phys.* **105**, 084112 (2009).

²⁰H. D. Li, C. D. Feng, and W. L. Yao, *Mater. Lett.* **58**, 1194 (2004).

²¹C. R. Zhou, X. Y. Liu, W. Z. Li, C. L. Yuan, and G. H. Chen, *J. Mater. Sci.* **44**, 3383 (2009).